Quadcopter Rotor Phasing for Minimization of Aircraft Vibratory Loads

Nicholas Kopyt
Undergraduate Research Assistant

Robert Niemiec
Research Scientist

Farhan Gandhi
Redfern Chair of Aerospace Engineering

Center for Mobility With Vertical Lift
Rensselaer Polytechnic Institute
Troy, NY, United States

ABSTRACT

Vibration reduction via individual rotor phasing is explored systematically on a 3.2kg quadcopter with stiff, variable-pitch rotors. Multi-rotor phase modes are defined and systematically examined in turn on both a cross- and plus-configuration quadcopter. 45° of pitch phasing reduces the 2/rev vertical vibrations by 97% from the case where all rotors are in-phase, from 0.13g to 0.004g, and 2/rev drag by 89.5% (from 0.06g to 0.0063g). 2/rev pitching moment is also reduced by 17% for $\Phi_P = 45°$, but cannot be reduced to zero for any Φ_P. Roll and yaw phasing can also reduce 2/rev vertical forces, but introduce significant roll vibration. Roll phasing also introduces a yaw moment, while differential phasing adds a 2/rev side force. None of the three modes defined on a plus-type quadcopter reduce all of the forces simultaneously.

INTRODUCTION

Electric Vertical Takeoff and Landing (eVTOL) vehicles have proliferated in recent years. The combination of extremely simple drive systems (often a single moving part per rotor) and the flexibility afforded by electric power distribution have reduced the barriers to entry into VTOL design. As a result, new designers ranging from hobbyists to startup companies have entered the field in addition to the large helicopter manufacturers.

Until recently, much of the analysis of eVTOLs has been limited to small-scale multicopters, and focused on algorithms for control. These analyses used very simple models to represent the rotor aerodynamics, most commonly assuming thrust and torque are explicitly proportional to the square of the rotor speed (Refs. 1,2). While these models are very lightweight and suited to control design of small eVTOLs, they are completely incapable of capturing rotor vibratory loads.

More recently, high-fidelity CFD analyses have been used to analyze the performance variety of eVTOL configurations. Yoon et. al (Ref. 3) examined the aerodynamics of small-scale UAS rotors using the RANS solver OVERFLOW and examined the effect vertical rotor placement had on the rotor-fuselage interactional aerodynamics in hover. Misiorowski et. al (Ref. 4) used the finite-element solver AcuSolve to predict rotor-rotor interference effects in forward flight. While CFD techniques provide excellent accuracy and can model complex aerodynamic interactions, it is ill-suited to parametric variation due to the computational expense associated with solving the Navier-Stokes equations.

Blade-element-theory-based models have also been used to predict the performance of multicopters. The comprehensive rotorcraft code CHARM was used to predict eVTOL tiltwing and tailsitter performance using prescribed wake and free wake aerodynamic models (Ref. 5). The authors previously (Ref. 6) applied the Hodges-Dowell elastic blade equations to a plastic rotor, finding that the introduction of blade elasticity to UAS-scale rotors significantly affected both steady and vibratory loads. These types of models represent a good compromise between model fidelity and computational expense, making them well-suited to parametric variation.

One major challenge in rotorcraft design is the vibration caused by the cyclic nature of rotor loads. As aerodynamic conditions on the blades change over the course of a revolution, the forces and moments experienced by any blade are periodic at harmonics of the rotational speed. Any vibrations, except those at a multiple of the blade passage frequency, are filtered out (assuming identical blades in steady-state operation), which reduces the vibration experienced the aircraft (Ref. 7). The stiff, two-bladed rotors commonly used on eVTOL aircraft are likely to experience large vibrations, as the 1/rev oscillations in dynamic pressure will introduce significant 2/rev drag, side force, pitching moment, and rolling moment in the non-rotating reference frame. There will also be a 2/rev change in the rotor thrust, coming from 2/rev changes in the lift on the rotor blades. Wind tunnel testing of plastic rotors (Ref. 8) revealed very large in-plane vibratory loads, with the 2/rev drag force greatly exceeding its steady value, acting on the same order as the mean rotor thrust.

Because the individual rotors of typical eVTOL designs are individually driven, the relative phase of rotors or subsets of rotors can be controlled, unlike mechanically-linked rotors. Schiller et. al (Ref. 9) explored the use of relative phasing of rotor pairs on an octocopter to reduce the acoustic profile. A similar study was performed by Pascioni and Rizzi (Ref. 10)

on the NASA GL-10 Greased Lightning, a tilt-wing configuration. Both of these studies used aircraft driven by fixed-pitch propellers, which must vary their speed to trim and control the aircraft, so their ability to regulate rotor phase is limited.

The objective of this study is to explore the concept of rotor phase control for the reduction of vibratory loads experienced by a nominal quadcopter. The relative phase of the rotors will be defined in terms of aircraft-level "modes," which will be parametrically varied to explore their effects on aircraft-level vibration. Quadcopters in both a "cross-configuration" and "plus-configuration" will be examined, and the differences in their vibratory forces and moments will be reported.

AIRCRAFT MODEL

The aircraft modeled in this study is the Straight-Up Imaging Endurance Quadcopter (Fig. 1). This 3.2kg quadcopter is equipped with by four 15-inch propellers made of Carbon Fiber Reinforced Polymer. The geometry of the rotor is taken from Russell and Sekula (Ref. 11), and is plotted in Fig. 2.

Table 1: Summary of aircraft parameters

Quadcopter Parameters	
Rotor Radius	7.5 in (0.1905 m)
Boom Length	12 in (0.3048 m)
Rotor Speed	3626 RPM (380 rad/s)
GTOW	7.04 lb (3.2 kg)

Fig. 1: Straight-Up Imaging (SUI) Endurance

To facilitate phase-control, the rotors are assumed to spin at identical speeds, and the typical RPM-control used on these multicopters is eschewed in favor of collective pitch control on the individual rotors. The aerodynamic characteristics of the airfoils are also taken to be identical to the baseline fixed-pitch rotor.

Rotor analysis is performed using the Rensselaer Multicopter Analysis Code (RMAC, Ref. 12), a blade-element-theory-based rotorcraft analysis code written to analyze multicopters. A 10-state Peters-He finite-state dynamic wake model is used on each rotor. The rotor blades are assumed to be rigid, justified by the stiffness of the carbon-fiber construction of the SUI Endurance Blades (Ref. 11).

The required root pitch of each individual rotor (and attitude) for trimmed flight is determined using RMAC. The control

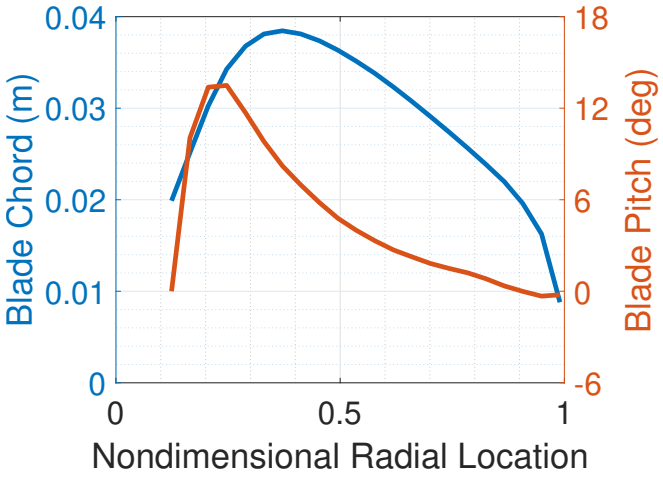

Fig. 2: SUI Endurance Rotor Geometry

inputs are defined using multi-rotor coordinates (Ref. 13). The multi-rotor coordinate transform uses the azimuthal locations of each rotor to determine a mixing matrix (Eq. 1), from which the individual rotor collective input can be obtained from the multi-rotor inputs. The azimuthal locations of the four rotors are also shown in Fig. 3.

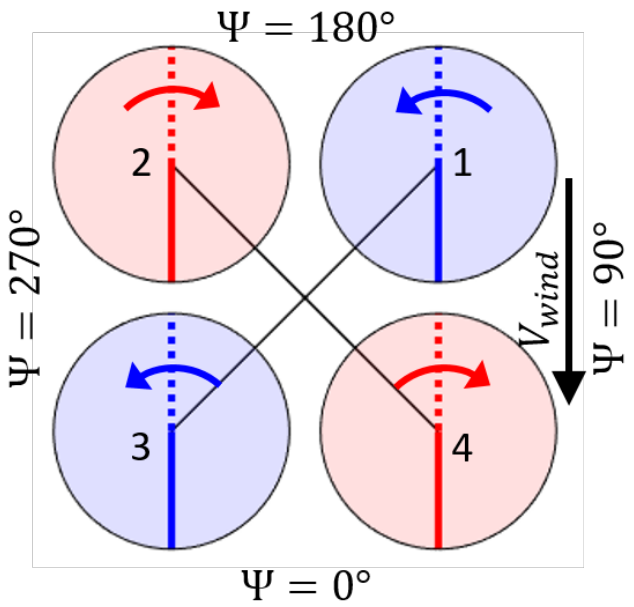

Fig. 3: Cross-configuration quadcopter with zero relative phasing between the rotors

$$\begin{bmatrix}\theta_1\\ \theta_2\\ \theta_3\\ \theta_4\end{bmatrix} = \begin{bmatrix}1 & \sin\Psi_1 & \cos\Psi_1 & -1\\ 1 & \sin\Psi_2 & \cos\Psi_2 & 1\\ 1 & \sin\Psi_3 & \cos\Psi_3 & -1\\ 1 & \sin\Psi_4 & \cos\Psi_4 & 1\end{bmatrix}\begin{bmatrix}\theta_0\\ \theta_{1s}\\ \theta_{1c}\\ \theta_d\end{bmatrix} \quad (1)$$

θ_0 represents the mean collective, and regulates the total thrust produced by the aircraft. θ_{1s} increases thrust produced by rotors on the right side of the aircraft, while reducing thrust on the left side, producing a roll-left moment. Similarly, θ_{1c} produces a nose-down moment by increasing the root pitch on

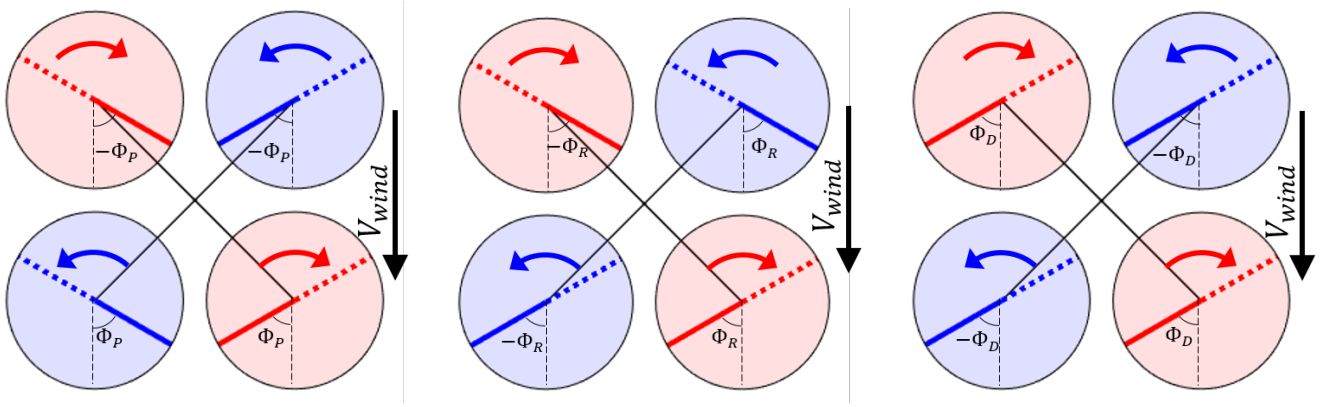

(a) Pitch Phasing, Φ_P (b) Roll Phasing, Φ_R (c) Differential Phasing, Φ_D

Fig. 4: Phasing Modes of a cross-configuration quadcopter

the rear rotors, relative to the front. Finally, θ_d decreases the pitch (and reaction torque) of the counter-clockwise (CCW) spinning rotors, and increases pitch of the clockwise (CW) spinning rotors, to induce a net nose-left yaw moment.

The relative rotor phasing is defined using a similar transform. The instantaneous orientation of each individual rotor, defined by the position of an arbitrary reference blade, can be obtained by using the transform in Eq. 2. The azimuth of a rotor is defined as zero when the reference blade extends downstream, and increases in the direction the rotor spins, such that $0^\circ < \psi <= 180^\circ$ is the advancing side of the rotor, and $180^\circ < \psi <= 360^\circ$ is the retreating side. The first column in Eq. 2 represents the mean rotor phase, and is equal to Ωt. By definition, this term adjusts the phase of all rotors equally, thus the relative phase between any two rotors remains unchanged. Because this term does not introduce any relative phasing between the rotors, it is not usable for vibration reduction.

$$\begin{bmatrix}\psi_1\\ \psi_2\\ \psi_3\\ \psi_4\end{bmatrix} = \begin{bmatrix}1 & 1 & -1 & -1\\ 1 & -1 & -1 & 1\\ 1 & -1 & 1 & -1\\ 1 & 1 & 1 & 1\end{bmatrix} \begin{bmatrix}\Phi_0\\ \Phi_R\\ \Phi_P\\ \Phi_D\end{bmatrix} \tag{2}$$

The remaining three columns in Eq. 2 introduce relative phasing between the rotors. Positive Φ_P (Fig. 4a) causes rotors on the rear to lead rotors on the front of the aircraft. Similarly, positive Φ_R causes the rotors on the right side of the vehicle to lead those on the left side, as depicted in Fig. 4b. Finally, Φ_D (Fig. 4c) introduces a phase between counter-clockwise-spinning and clockwise-spinning rotors, with the former lagging the latter.

RESULTS

Isolated Rotor Forces and Moments

For an edgewise rotor in forward flight, the in-plane component of velocity through the rotor disk introduces a 1/rev variation in dynamic pressure. At the same time, the longitudinal

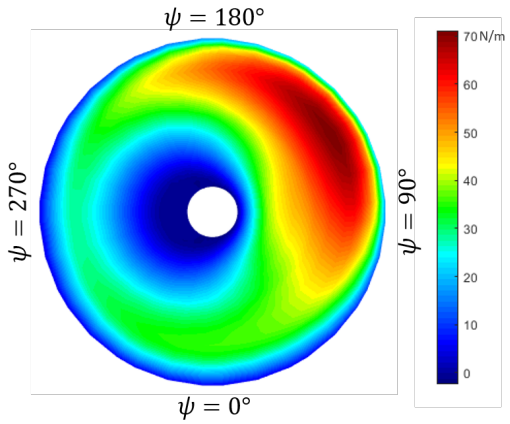

Fig. 5: Lift distribution on Rotor 1 (CCW) trimmed at 13 m/s

inflow distribution increases the angle of attack on the front of the disk, resulting in the lift distribution shown in Fig. 5. Integrating the lift across the span of any blade produces the blade root vertical shear, shown versus azimuth in Fig. 6. Each of the two identical blades produce a 1/rev dominant signal, but due to the 180° phasing between the blades, they are out-of-phase. The result of the summation of the individual root shears is a 2/rev-dominant vertical vibration on the rotor hub, shown in black in Fig. 6.

The lift distribution also produces a blade-root flapping moment, dominantly 1/rev. In the non-rotating reference frame, this results in a 2/rev hub rolling and pitching moment.

The rotor drag distribution is plotted in Fig. 7. The higher dynamic pressure on the advancing side, coupled with high pitch and chord inboard result in a large drag in the mid-span section of the blade near $\psi = 90^\circ$. The 1/rev blade root drag shear results in a 2/rev drag and side force acting at the rotor hub, which is transmitted to the airframe.

Cross-Configuration Quadcopter

Aircraft Trim Fig. 8 shows the individual rotor pitch inputs for the cross-configuration quadcopter in forward flight. In

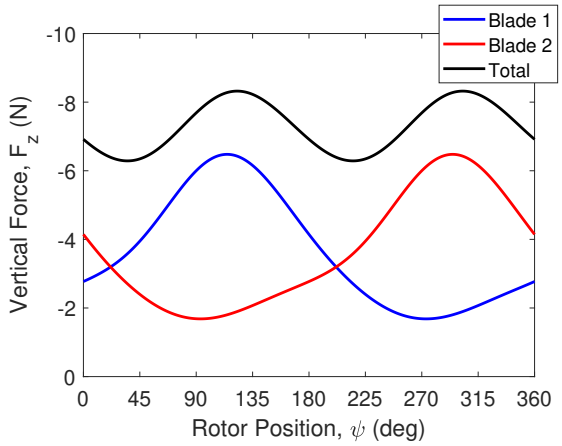

Fig. 6: Blade root and hub vertical on Rotor 1 trimmed at 13 m/s

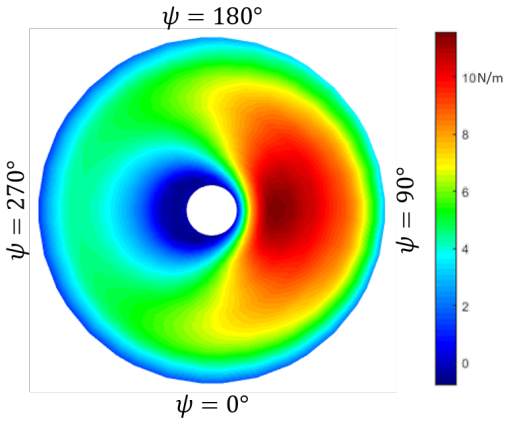

Fig. 7: Drag force distribution on Rotor 1 (CCW) trimmed at 13 m/s

hover, all four rotors have the same pitch, which decreases slightly at moderate speed before increasing at higher speeds. A differential pitch between the front and rear rotors is also enforced in forward flight, as the rear rotors must produce additional thrust to counteract the nose-up hub moments produced by each rotor.

Consider first a baseline case where all rotors are in-phase, the individual 2/rev vertical and drag forces from each rotor are in-phase and interfere constructively at the aircraft level. The side forces produced by the two front rotors are equal in magnitude, but opposite in sign, as these two rotors are mirrors of one another. The same argument holds for the rear rotors, and thus the net side force on the aircraft is identically zero.

There are two sources vibratory of pitching moment at the aircraft-level—rotor hub pitching moments, which (for a two-bladed rotor) are caused by front-rear asymmetry in the rotor lift distribution, and induced pitching moments, due to rotor thrust with a moment arm. Mirroring the rotors about the aircraft XZ-plane does not affect the hub pitching moment produced by an individual rotor, so all four rotors produce a vibratory pitching moment in-plane. With all four rotors in-phase, these hub-pitching moments interfere constructively. However, because the front rotors' thrust is in-phase with that of the rear rotors, the induced moments interfere destructively.

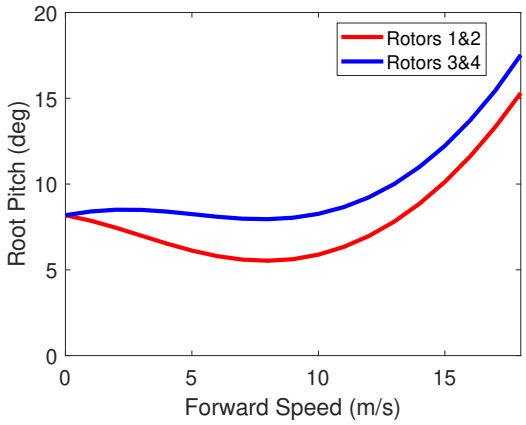

Fig. 8: Trim collective-pitch requirements for cross-configuration quadcopter

Hub rolling moments cancel similarly to the side forces as the hub rolling moment of the front right rotor is exactly out-of-phase with that of the front left (this is also the case for the rear rotor pair). The induced rolling moment of the right rotors opposes the induced rolling moment of the left rotors which results in a complete cancellation of the rolling moments at the aircraft C.G..

The vibratory hub yawing moments are harder to predict and neglected in this study. Thus, the only source of aircraft-level yawing moment is induced by the drag and side forces of each rotor. In the baseline phasing (Fig. 3), the induced yawing moment cancels as a result of the induced moments from the drag forces of the left rotor pair exactly counteracting the right rotor pair and the induced moments of side forces of the clockwise rotors exactly canceling the counter-clockwise rotors.

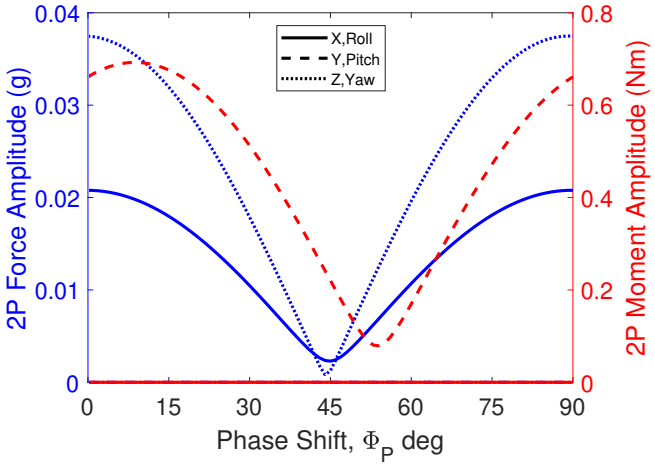

Fig. 9: Amplitude of 2/rev vibratory forces and moments about the aircraft C.G. using pitch phasing (V = 5m/s)

Pitch Phasing For a pure pitch phasing (Φ_P, Fig. 4a), the front two rotors will lag and the rear two rotors will lead rel-

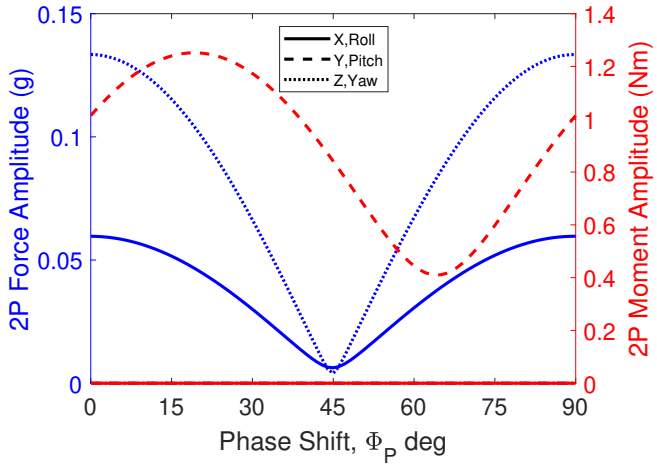

Fig. 10: Amplitude of 2/rev vibratory forces and moments about the aircraft C.G. using pitch phasing (V = 13m/s)

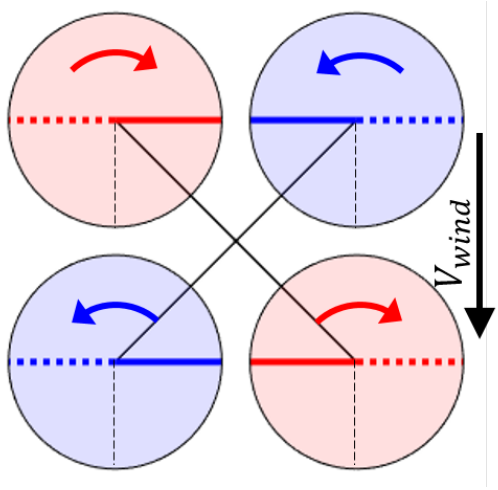

Fig. 11: Cross-configuration quadcopter with $\Phi_P = 90°$

ative to the baseline. This results in a relative phase difference between the front and rear rotors of $2\Phi_P$. Figs. 9 and Fig. 10 show the amplitude of the forces and moments exerted on the aircraft center of gravity for a phase shift of Φ_P at 5 and 13 m/s cruise speed respectively. The left axis corresponds to the 2/rev vibratory forces normalized by the aircraft weight (representing an acceleration measured in g) and the right axis corresponds to the amplitude of the 2/rev moments ($N\ m$). Comparing the scales of Figs. 9 and 10, it is clear that increased forward speed results in higher-amplitude vibration, as well as a change in the relationship between vibratory pitch moment and Φ_P.

The 90° periodicity of Φ_P is a function of the number of blades. At $\Phi_P = 90°$, the front two rotors will lead from the initial position by 90°, and the rear two rotors will lag by 90° (Fig. 11). This results in a relative phase difference between the front and rear rotors of exactly 180° ($2\Phi_P$) which is equivalent to relative phase difference of 0° for a two-bladed rotor.

Regardless of the value of Φ_P, the two front rotors remain in-phase with one another. Therefore, the forces and moments at the hubs of these-two rotors always have the same magnitude. As a consequence, those forces and moments that do not depend on the rotor spin direction (namely rotor thrust, drag, and hub pitching moment) always compound, while those that change sign based on the spin direction (side force and hub rolling moment) always cancel. A similar argument holds for the two rear rotors. Therefore, for all values of Φ_P, the aircraft-level 2P side-force, rolling moment, and yawing moment, are zero.

Because the front two rotors' thrust and drag remain in-phase for all Φ_P, changing the value of Φ_P changes the aircraft-level vertical and drag vibratory forces by changing the relative phase of these two rotors loads relative to those of the two rear rotors, as shown in the top row of Fig. 12. For $\Phi_P = 0°$ or 90°, all four rotors are in-phase, and so the resulting aircraft-level vertical vibration has an amplitude of 0.13g. As the phase increases from 0°, the front rotors' thrust lags the rear rotors' thrust, resulting in destructive interference. At $\Phi_P = 45°$, the 2/rev vibratory loads are perfectly out-of-phase, resulting in minimum vibration. Due to the small differences in the rotor pairs' thrusts, some 2/rev vibration remains, but is reduced by 97% (to 0.004g).

Aircraft-level pitching moments have two fundamental sources: the hub pitching moments, transmitted through the frame of the aircraft; and the moments induced by the thrust produced at the rotor hub, offset by a moment arm (drag-induced pitching moment is negligible). These two contributors are plotted against Φ_0 in the first and second rows of Fig. 13, respectively. For either $\Phi_P = 0°$ or 90°, the hub pitching moments are all in-phase, and sum to produce a large overall pitching moment at the C.G. However, the moments induced by the rotor forces, dominated by the thrust, are out-of-phase. This is because the rotor thrusts themselves are in-phase (Fig. 10) and the fact that these two pairs of rotors are on opposite sides of the pitching axis.

Conversely, when $\Phi_P = 45°$, the hub-pitching moments are out-of-phase, and interfere destructively, while the induced moments are interfering constructively. Because the rotor thrusts are out-of-phase for $\Phi_P = 45°$, the thrust-induced moments are in-phase. Overall, the total pitching moment at the C.G. (plotted in the third row of Fig. 13) shows the smallest magnitude for $\Phi_P = 60°$, where the thrust-induced and hub pitching moments are mostly out-of-phase.

Roll Phasing For the quadcopter in and cross-configuration, Φ_R causes the rotors on the right side of the aircraft to lead those on the left side of the aircraft, as shown in Fig. 4b. The amplitude of the 2/rev forces and moments are periodic every 90°, similar to pitch phasing (Fig. 14). However, aside from the rotor thrust and drag, which behave similarly to the Φ_P case, except exchanging front/rear rotor pairing for left/right rotor pairing, all of the forces and moments behave qualitatively differently.

When varying Φ_R, the two rotors on the right side of the aircraft remain in-phase. Therefore, these two rotors' thrust also remain in-phase. As these two rotors are on opposite sides of the pitching axis, this causes their induced pitching moments

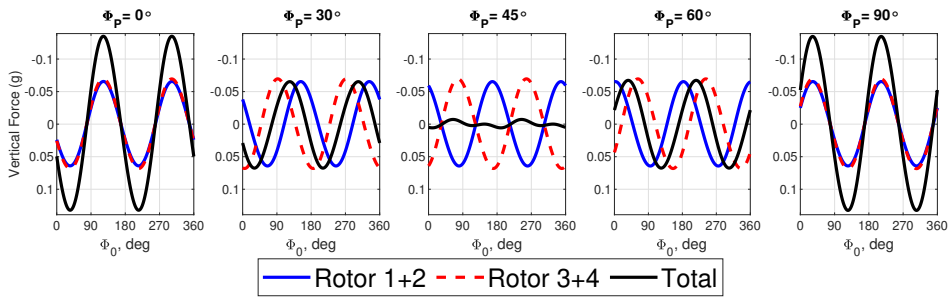

Fig. 12: 2/rev vibratory vertical rotor forces using Pitch Phasing (V = 13m/s)

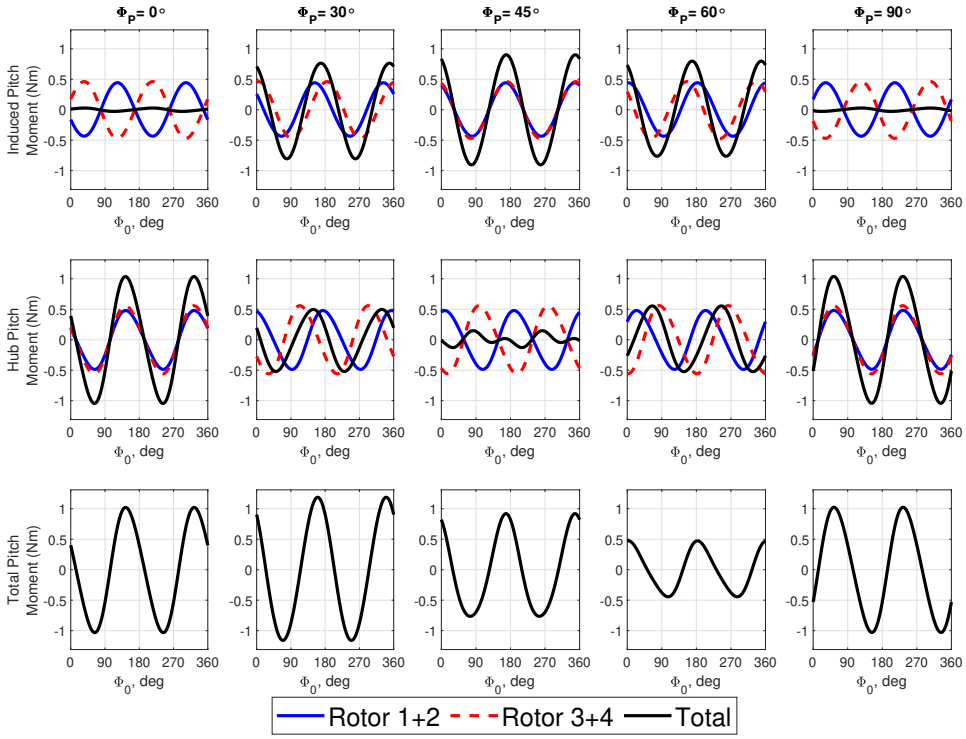

Fig. 13: 2/rev vibratory pitching moments using Pitch Phasing (V = 13m/s)

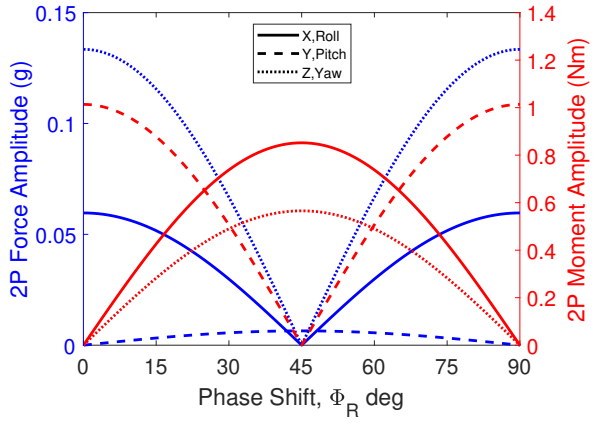

Fig. 14: Amplitude of 2/rev vibratory forces and moments about the aircraft C.G. using Roll Phasing

to remain out-of-phase for all Φ_R. With only the hub pitching moments sensitive to Φ_R, the overall pitching vibration is reduced to near zero by setting $\Phi_R = 45°$.

However, unlike Φ_P, introduction of Φ_R causes the 2/rev aircraft rolling moments to be nonzero. Like the pitching moments, both hub moments and force-induced moments are transmitted to the aircraft center of gravity, which are plotted in Fig. 15. At $\Phi_R = 0°$ and $\Phi_R = 180°$, the thrust-induced rolling moments are out-of-phase, resulting in their cancellation. At $\Phi_R = 45°$, the rotor 2/rev thrust is out-of-phase, and so the induced rolling moment is in-phase. The hub moments are also in-phase at $\Phi_R = 45°$, but are smaller than the thrust-induced moments, which dominate the overall rolling moment at the C.G.

Finally, consider the yaw moment experienced at the C.G., which also contains a 2/rev hub torque and moments induced by 2/rev drag and side force on the rotors. The former is diffi-

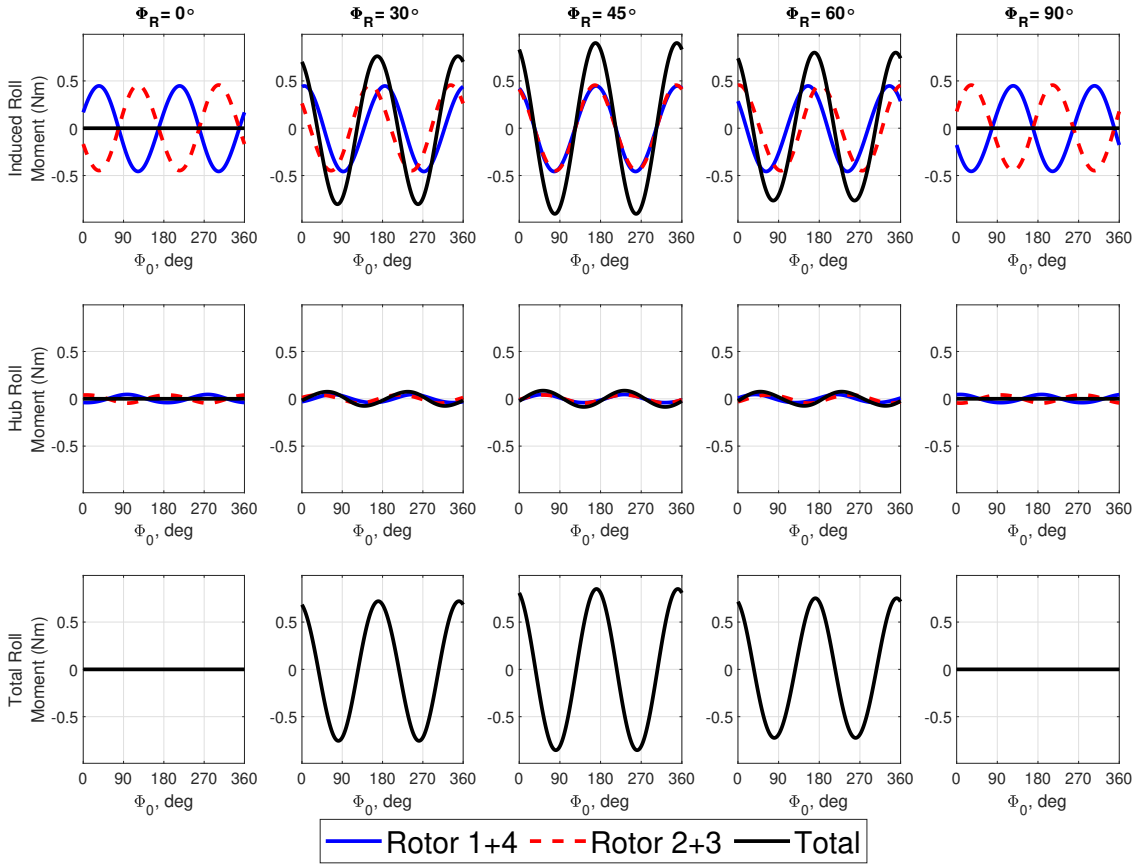

Fig. 15: 2/rev vibratory rolling moments using Roll Phasing (V = 13m/s)

cult to predict, and is neglected in this analysis, but the latter has a significant effect on the overall moments, which is maximized when the left and right rotors are out-of-phase with one another, similar to the thrust-induced pitching and rolling moments.

Differential Phasing The differential shift mode adjusts the relative phase between rotors of opposite spin directions; all CW spinning rotors will lead where the CCW spinning rotors will all lag by the same amount. The forces and moments at the C.G. when applying Φ_D are plotted in Fig. 16. Like pitch and roll phasing, the 2/rev drag and thrust are minimized when the rotors are 90° out-of-phase, corresponding to $\Phi_D = 45°$.

The biggest difference between vibratory loads with differential phasing relative to roll phasing is the magnitude of the side force, which becomes large near $\Phi_D = 45°$. At $\Phi_D = 45°$, the side force magnitude of the CCW rotors will reach their maximum as that of the CW rotors reaches its minimum. Because the direction of the side force is dependent on the rotor spin direction, the CCW rotors interfere constructively with the CW rotors.

At first glance, the roll moment appears to behave similarly with Φ_D as it does with Φ_R. However, there is a key difference: the magnitude is 35% larger when $\Phi_D = 45°$ than when $\Phi_R = 45°$. Consider the two CCW rotors, located at the front-right and rear-left of the aircraft. These two rotors are always in-phase, and so their thrust-induced moments must similarly be in-phase. Similarly, the two CW rotors are also in-phase. Therefore, any vibratory moment must be caused by hub rolling moments, which are out-of-phase when $\Phi_D = 45°$.

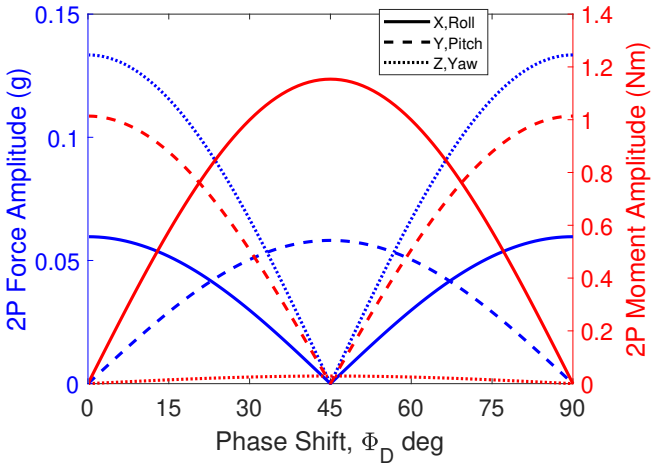

Fig. 16: Amplitude of 2/rev vibratory forces and moments about the aircraft C.G. using Differential Phasing

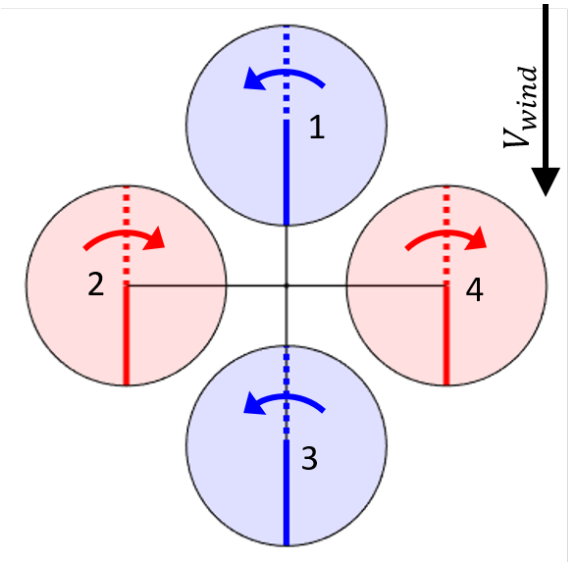

Fig. 17: Plus-configuration quadcopter with no relative phase between rotors

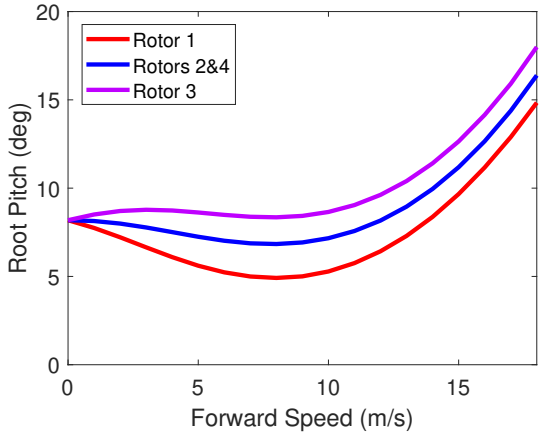

Fig. 18: Plus-configuration trim sweep

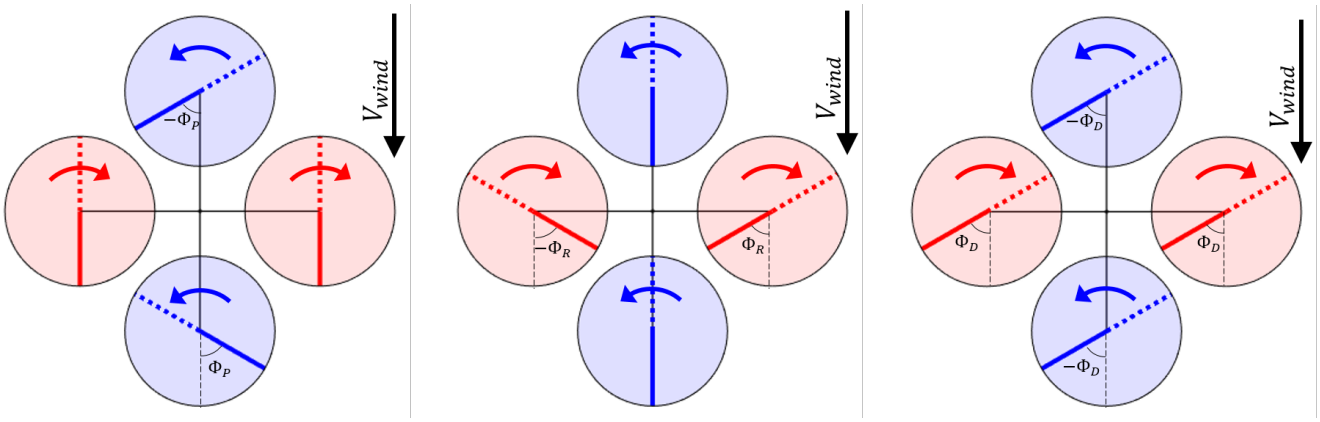

(a) Pitch Phasing, Φ_P (b) Roll Phasing, Φ_R (c) Differential Phasing, Φ_D

Fig. 19: Phasing modes of a plus-configuration quadcopter

Plus-Configuration Quadcopter

Aircraft Trim The quadcopter in a plus-configuration (Fig. 17) has three distinct collective pitch controls (unlike the cross-configuration, which has only two). The left and right rotors operate at identical collective pitch settings while the front and rear rotors respectively have lower and higher pitch settings, as shown in Fig. 18. This is a result of the requirement of rear rotor to produce more thrust than the front rotor in order to counteract the nose-up pitching moment produced by the rotors in forward flight.

As the locations of the rotors have changed, the multi-rotor coordinate transform has also changed. Individual rotor phasing can now be obtained from Eq. 3, and the phasing modes are visualized in Fig. 19.

$$\begin{bmatrix}\psi_1\\ \psi_2\\ \psi_3\\ \psi_4\end{bmatrix} = \begin{bmatrix}1 & -1 & 0 & -1\\ 1 & 0 & -1 & 1\\ 1 & 1 & 0 & -1\\ 1 & 0 & 1 & 1\end{bmatrix}\begin{bmatrix}\Phi_0\\ \Phi_P\\ \Phi_R\\ \Phi_D\end{bmatrix} \tag{3}$$

Pitch Phasing One difference from the cross-configuration quadcopter is the change in periodicity from 90° to 180°. For the plus-configuration, the phase of the side rotors remains unchanged for all Φ_P, the front rotor leads by Φ_P and the rear rotor lags by Φ_P. As a consequence, the relative phases between rotors will not return to its initial state until the relative phase between all rotors is a multiple of the blade spacing. For $\Phi_P = 90°$, the relative phase between the front and side rotors is only 90° (Fig. 20). Doubling Φ_P will produce a 360° phase difference between the front and rear rotor as well as a 180° difference between the front and side rotors. This condition is identical to the original condition ($\Phi_P = 0°$). Consequently,

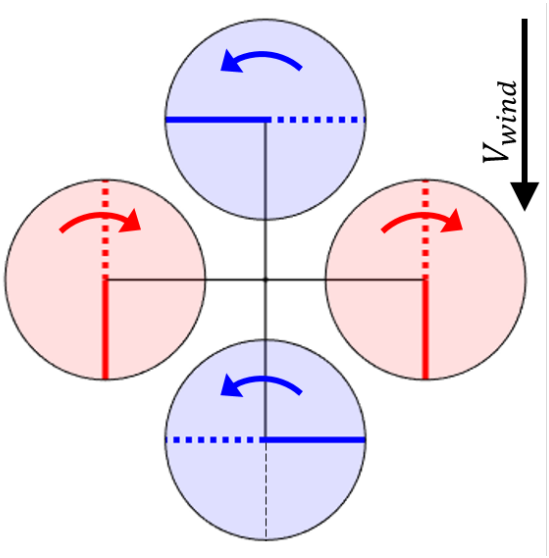

Fig. 20: Plus-configuration quadcopter with $\Phi_P = 90°$

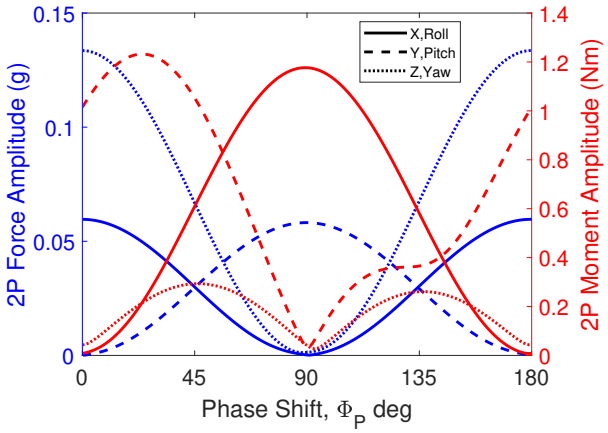

Fig. 21: Amplitude of 2/rev vibratory forces and moments about the aircraft C.G. using Φ_P mode

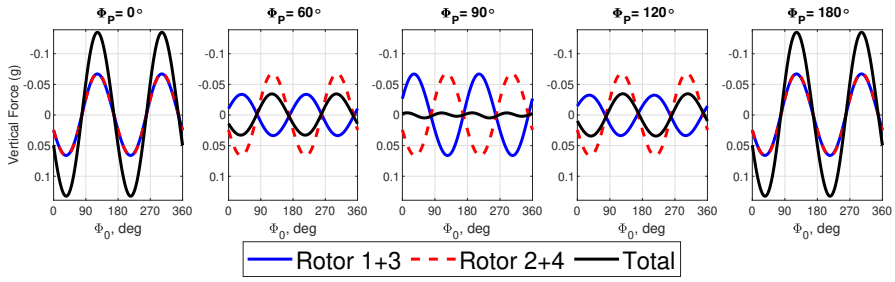

Fig. 22: 2/rev vibratory vertical rotor forces using Pitch Phasing (V = 13m/s)

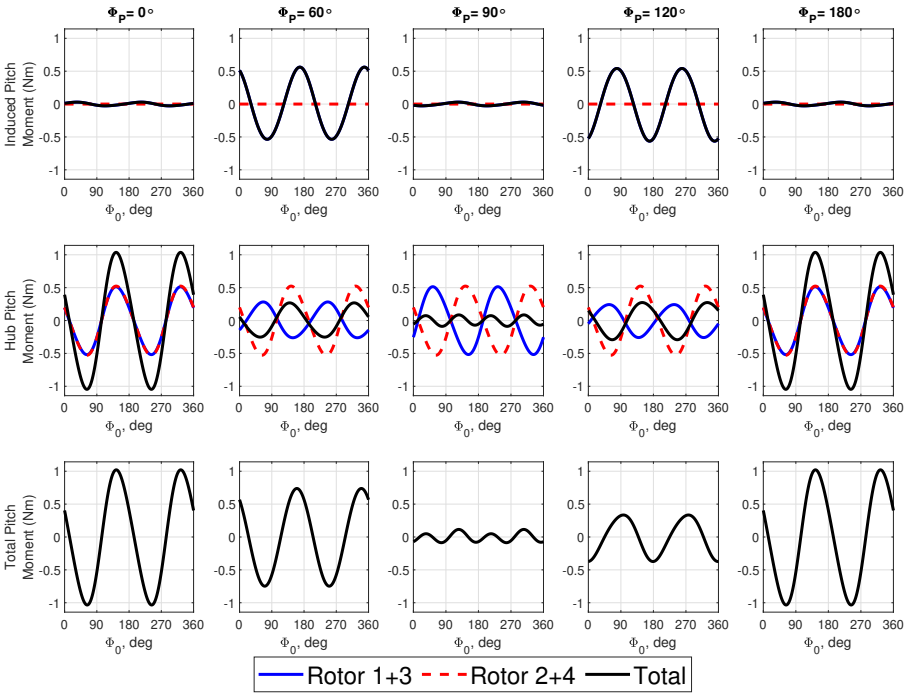

Fig. 23: 2/rev vibratory induced pitching moments using Pitch Phasing (V = 13m/s)

the periodicity of the vibratory force and moment magnitude is periodic with respect to Φ_P with a period of 180° (Fig. 21).

Since the relative phase of the two side rotors is unaffected by this mode, the 2/rev forces produced by these rotors always remains in-phase. As a consequence, the forces will only cancel if the front and rear rotors are out-of-phase with the side rotors. For $\Phi_P = 90°$, the vertical and drag forces of the front and rear rotors are both in-phase with each other and out-of-phase (Fig. 22).

Unlike the cross-configuration, the vibratory side forces become significant as a result of pitch phasing. The side forces of the left and right rotors always constructively interfere for this phasing mode, and the side forces of the front and rear rotors begin out-of-phase with the side rotors at $\Phi_P = 0°$. For $\Phi_P = 90°$, the side forces of the front and rear rotors become in-phase with the side rotors, and compound to create a relatively large 2/rev side-force. (Fig. 21).

The 2/rev induced roll moment is only affected by the side rotors since the front and rear rotors are coincident with the roll axis. Since the thrust of the two side rotors remains in-phase for all Φ_P, the induced roll moment always cancels. Thus, only the hub rolling moments can contribute to aircraft-level roll vibrations. The hub rolling moments of the side rotors also remain in-phase for all Φ_P. However, the phase between the hub moments of the front and rear rotors are affected. At $\Phi_P = 0°$, these two rotors' hub moments are in-phase with each other, and out-of-phase with the left and right rotors, resulting in a net cancellation. At $\Phi_P = 90°$, the front and rear rotors 2/rev hub moments are out-of-phase with one another, and cancel. This, in turn leaves the 2/rev moments from the left and right rotors unaffected, and the net 2/rev rolling moment is greatest.

The 2/rev pitching moments on the plus-configuration quadcopter are broken down in Fig. 23. Considering the induced moments, the net moments are zero when $\Phi_P = 0°$, 90°, or 180°. This is because the only two rotors that can contribute to induced moments (the front and rear) are in-phase at these values of Φ_P. When Φ_P takes any other value, a 2/rev induced pitching moment exists. All four rotors contribute to the total hub pitching moment and are all in-phase at $\Phi_P = 0°$ or 180°. At $\Phi_P = 90°$, the hub pitching moment of the front and rear rotors are out-of-phase with the left and right, leading to cancellation of the 2/rev hub pitching moment. The total 2/rev pitching moment is obtained by summing the induced and hub pitching moments, resulting in the bottom row of Fig. 23. At $\Phi_P < 90°$, the induced moments are largely in-phase with the hub moments, while they are largely out-of-phase for $\Phi_P > 90°$, resulting in the asymmetry in Fig. 21.

The 2/rev yawing moment amplitude has local minima at $\Phi_P = 0°$, $\Phi_P = 90°$ and $\Phi_P = 180°$ with maxima in at $\Phi_P = 45°$ and 135°. The force-induced yaw moments have two sources: drag on the left/right rotors, and side-force on the front/rear rotors. The former is not affected by Φ_P—the drag is always in-phase, which leads to cancellation of their induced yaw moment. When the front and rear rotors are out-of-phase ($\Phi_P = 45°$ or 135°), these side-forces are similarly out-of-phase, and since these rotors are on opposite sides of the C.G., their induced yaw moments are in-phase.

Roll Phasing

Similar to Φ_P, Φ_R is also periodic every 180° as a result of the three unique phase angles when using this mode. The behavior of the 2/rev C.G. force amplitude is identical to Φ_P, with minima for thrust/drag and a maximum for side force occurring at $\Phi_R = 90°$ (Fig. 24).

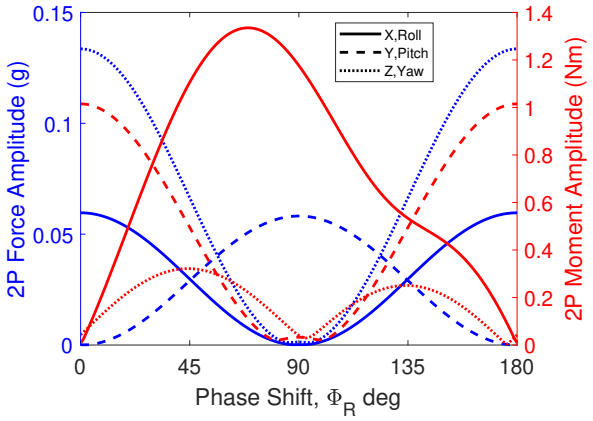

Fig. 24: Amplitude of 2/rev vibratory forces and moments about the aircraft C.G. using Φ_R mode

The induced pitching moment on the aircraft is only dependent on the thrust of the front and rear rotors. For all values of Φ_R, the vertical forces of the front and rear rotors remain in-phase since this phasing mode only adjusts the relative phasing of the side rotors. As a result, the induced pitching moments interfere destructively for all values of Φ_R and any changes in the 2/rev pitching moment in Fig. 19b must be a function of only the hub moments. Like the hub rolling moments generated by the side rotors in the pitch phasing mode, the front and rear rotor hub pitching moments in the roll phasing mode constructively interfere for all Φ_R. The hub pitching moments of the side rotors must be in-phase with each other and out-of-phase with the front and rear rotors in order for a cancellation to occur. At $\Phi_R = 90°$, the hub moments will cancel, leaving only a small 2/rev pitching moment (Fig. 24) that exists due to the difference in 2/rev thrust between the front and rear rotors.

Fig. 25 shows the change in the induced and hub rolling moments as Φ_R is changed. In a manner similar to the induced pitching moment with Φ_P, the induced rolling moment is zero for $\Phi_R = 0°$, 90°, and 180°. The hub rolling moments are out-of-phase for $\Phi_R = 0°$ and 180°, and in-phase for $\Phi_R = 90°$. Though the hub pitching moments are symmetric about $\Phi_R = 90°$ (middle row of Fig. 25), the induced moments are not, resulting in an asymmetry in roll moment in Fig. 24.

The yaw moment behaves similarly to Φ_P, except that it is the left and right rotors' drag that dominate the behavior, as

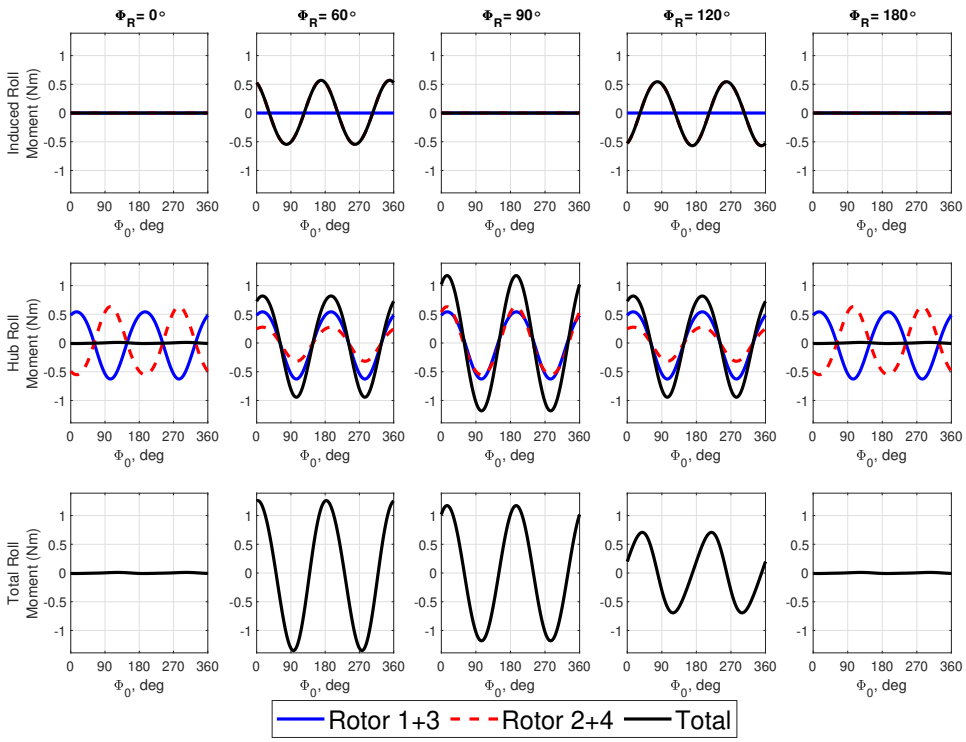

Fig. 25: 2/rev vibratory rolling moments using Roll Phasing (V = 13m/s)

the front rotor's forces are always in-phase with the rear rotor. At any point where the left and right rotors' drag are in-phase ($\Phi_R = 0°, 90°$ or $180°$), the net induced yaw moment is nearly zero, and at each point where their drag is out-of-phase ($\Phi_R = 45°$, $\Phi_R = 135°$), the induced yaw moment is maximum.

Differential Phasing

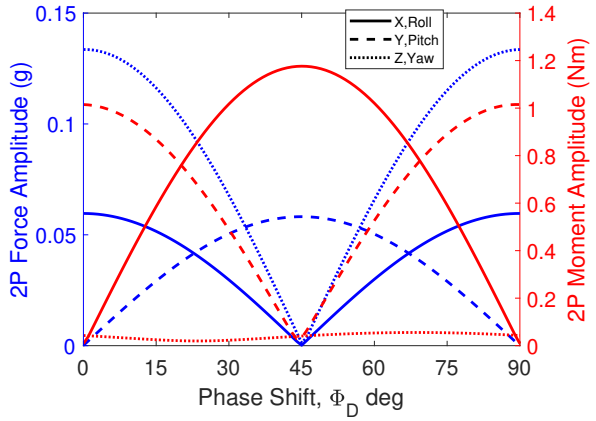

Fig. 26: Amplitude of 2/rev vibratory forces and moments about the aircraft C.G. using Φ_D mode

Differential phasing is essentially the same between the cross- and plus-configurations (compare Eqs. 2 and 3), causing the CCW rotors to lag the CW rotors. Additionally, comparing the aircraft-level vibration magnitudes for the plus-configuration in Fig. 26 to the cross-configuration in Fig. 16 shows that the two types behave similarly as Φ_D is changed.

CONCLUSIONS

A 3.2kg cross- and plus-configuration quadcopter with variable-pitch rotors was trimmed in forward flight, and the vibratory forces and moments at the aircraft C.G. were calculated from the individual blade loads. Rotor phasing was defined in terms of three aircraft-level modes, using a linear transform to calculate the relative phase of any individual rotor.

The sensitivity of C.G. loads to rotor phasing was systematically explored using the three phase modes. For the cross-type quadcopter, pitch phasing can simultaneously minimize all 2/rev forces and moments at $\Phi_P = 45°$, except for pitch moment, which at maximized at this phasing. 2/rev pitching moment cannot be brought to zero at any value of Φ_P, due to the simultaneous variation of thrust-induced and hub pitching moments from individual rotors. Roll phasing allows cancellation of pitching moment, but introduces a roll moment of similar magnitude and a net 2/rev yaw moment. Differential phasing can similarly cancel pitch, but introduces a larger roll moment, as well as a 2/rev side force. All phase modes exhibited 90° periodicity.

On the plus-type quadcopter, the phase modes are defined such that only two rotors are impacted by pitch and roll phasing, which leads to a 180° periodicity with respect to these modes. Unlike the cross-type quadcopter, pitch phasing introduces 2/rev side force, rolling moment, and yawing moment

when nonzero. Rolling moment and side force are maximized when $\Phi_P = 90^\circ$, which minimizes the other forces and moments. Pitch moment is asymmetric about 90° due to phase differences between the thrust-induced and hub pitching moments.

Roll phasing on the plus-type quadcopter is similar to pitch phasing (on the same configuration), in that a side-force and rolling moment are large near $\Phi_R = 90^\circ$, while the other forces and moments are small. Differential phasing is very similar between the cross- and plus-configurations, due to the similar definitions of this mode.

REFERENCES

[1]Bouabdallah, S. and Siegwart, R., "Full Control of a Quadcopter," Proceedings of the 2007 IEEE/RSJ International Conference on Intelligent Robots and Systems, San Diego, CA, oct 2007.

[2]Fresk, E. and Nikolakopolous, G., "Full Quaternion Based Attitude Control for a Quadrotor," 2013 European Control Conference, Zürich, Switzerland, July 2013.

[3]Yoon, S., Diaz, P. V., Jr., D. D. B., Chan, W. M., and Theodore, C. R., "Computational Aerodynamic Modeling of Small Quadcopter Vehicles," American Helicopter Society 73rd Annual Forum, Fort Worth, TX, May 2017.

[4]Misiorowski, M., Gandhi, F., and Oberai, A., "A Computational Study on Rotor Interactional Effects for a Quadcopter in Edgewise Flight," American Helicopter Society 74th Annual Forum, Phoenix, AZ, May 2018.

[5]Quackenbush, T., Wachspress, D., Whitehouse, G., and Yu, M., "Analysis Methods for Tilting Wing and Tailsitter e-VTOL configurations," Vertical Flight Society Autonomous VTOL Technical Meeting and Electric VTOL Symposium, Mesa, AZ, Jan 2019.

[6]Niemiec, R. and Gandhi, F., "Effect of Elastic Blade Deformation on Trim and Vibratory Loads of a Quadcopter," American Helicopter Society 73rd Annual Forum, Fort Worth, TX, May 2017.

[7]Johnson, W., Cambridge University Press, New York, NY, 2013, pp. 717–722.

[8]Russell, C., Jung, J., Willink, G., and Glasner, B., "Wind Tunnel and Hover Performance Test Results for Multicopter UAS Vehicles," American Helicopter Society 72nd Annual Forum, West Palm Beach, FL, May 2016.

[9]Schiller, N., Pascioni, K., and Zawodny, N., "Tonal Noise Control using Rotor Phase Synchronization," Vertical Flight Society 75th Annual Forum, Philadelphia, PA, May 2019.

[10]Pascioni, K. and Rizzi, S., "Tonal Noise Prediction of a Distributed Propulsion Unmanned Aerial Vehicle," Paper AIAA 2018-3847, 24th AIAA/CEAS Aeroacoustics Conference Proceedings, Atlanta, GA, June 2018.

[11]Russell, C. and Sekula, M., "Comprehensive Analysis Modeling of Small-Scale UAS Rotors," American Helicopter Society 73rd Annual Forum, Fort Worth, TX, May 2017.

[12]Niemiec, R. and Gandhi, F., "Development and Validation of the Rensselaer Multicopter Analysis Code (RMAC): A Physics-Based Comprehensive Modeling Tool," Vertical Flight Society 75th Annual Forum, Philadelphia, PA, May 2019.

[13]Niemiec, R. and Gandhi, F., "Multi-rotor Coordinate Transforms for Orthogonal Primary and Redundant Control Modes for Regular Hexacopters and Octocopters," 42nd European Rotorcraft Forum, Lille, France, Sep 2016.